

Comparison of the magnetic properties of GeMn thin films through Mn L-edge x-ray absorption

S. Ahlers, P. R. Stone, N. Sircar, E. Arenholz, O. D. Dubon et al.

Citation: *Appl. Phys. Lett.* **95**, 151911 (2009); doi: 10.1063/1.3232245

View online: <http://dx.doi.org/10.1063/1.3232245>

View Table of Contents: <http://apl.aip.org/resource/1/APPLAB/v95/i15>

Published by the [American Institute of Physics](http://www.aip.org).

Related Articles

EXAFS Debye-Waller factors issued from Car-Parrinello molecular dynamics: Application to the fit of oxaliplatin and derivatives

JCP: BioChem. Phys. **7**, 02B612 (2013)

Communication: Influence of graphene interlayers on the interaction between cobalt phthalocyanine and Ni(111)

J. Chem. Phys. **138**, 081101 (2013)

EXAFS Debye-Waller factors issued from Car-Parrinello molecular dynamics: Application to the fit of oxaliplatin and derivatives

J. Chem. Phys. **138**, 084303 (2013)

Spectroscopic properties and quantum cutting in Tb³⁺–Yb³⁺ co-doped ZrO₂ nanocrystals

J. Appl. Phys. **113**, 073105 (2013)

Extended X-ray absorption fine structure study of mixed-ligand copper(II) complexes having analogous structures

J. Appl. Phys. **113**, 073701 (2013)

Additional information on *Appl. Phys. Lett.*

Journal Homepage: <http://apl.aip.org/>

Journal Information: http://apl.aip.org/about/about_the_journal

Top downloads: http://apl.aip.org/features/most_downloaded

Information for Authors: <http://apl.aip.org/authors>

ADVERTISEMENT

AIP | Applied Physics
Letters

EXPLORE WHAT'S NEW IN APL

SUBMIT YOUR PAPER NOW!

SURFACES AND INTERFACES
Focusing on physical, chemical, biological, structural, optical, magnetic and electrical properties of surfaces and interfaces, and more...

ENERGY CONVERSION AND STORAGE
Focusing on all aspects of static and dynamic energy conversion, energy storage, photovoltaics, solar fuels, batteries, capacitors, thermoelectrics, and more...

Comparison of the magnetic properties of GeMn thin films through Mn *L*-edge x-ray absorption

S. Ahlers,¹ P. R. Stone,^{2,3} N. Sircar,¹ E. Arenholz,⁴ O. D. Dubon,^{2,3} and D. Bougeard^{1,a)}

¹Walter Schottky Institut, Technische Universität München, Am Coulombwall 3, D-85748 Garching, Germany

²Department of Materials Science and Engineering, University of California, Berkeley, California 94720, USA

³Lawrence Berkeley National Laboratory, Berkeley, California 94720, USA

⁴Advanced Light Source, Lawrence Berkeley National Laboratory, Berkeley, California 94720, USA

(Received 12 August 2009; accepted 27 August 2009; published online 16 October 2009)

X-ray absorption spectroscopy of epitaxial GeMn thin films reveals an experimentally indistinguishable electronic configuration of Mn atoms incorporated in Ge_{1-x}Mn_x nanoclusters and in precipitates of the intermetallic compound Mn₅Ge₃, respectively. However, the average magnetic response of thin films containing Ge_{1-x}Mn_x nanoclusters is lower than the response of films containing Mn₅Ge₃ precipitates. This reduced magnetic response of Ge_{1-x}Mn_x nanoclusters is explained in terms of a fraction of Mn atoms being magnetically inactive due to antiferromagnetic coupling or the presence of structural disorder. A determination of the role of magnetically inactive Mn atoms in the self-assembly of the thermodynamically metastable Ge_{1-x}Mn_x nanoclusters seems to be an essential ingredient for an enhanced control of this promising high Curie temperature magnetic semiconductor. © 2009 American Institute of Physics. [doi:10.1063/1.3232245]

The material system Ge–Mn represents a promising candidate for magnetic semiconductor applications due to its compatibility to mainstream Si technology and the accessibility of Curie temperatures above room temperature.^{1–3} The latter was observed in epitaxially fabricated GeMn thin films, where specific epitaxy conditions far from thermodynamic equilibrium lead to an inhomogeneous distribution of Mn in the Ge host in the form of self-assembled, nanometer-sized, Mn-rich regions coherently embedded in the Ge-rich host matrix.^{1,4} In addition to such thermodynamically metastable Ge_{1-x}Mn_x nanoclusters, a small number of Mn_xGe_y intermetallic compounds are known, like, for example, Mn₅Ge₃. Mn₅Ge₃ is a magnetically hard compound⁵ with a Curie temperature near room temperature⁶ and a hexagonal lattice structure.⁷ Proper control of the epitaxy conditions in the GeMn material system allows the deposition of layers containing only Ge_{1-x}Mn_x nanoclusters, Mn₅Ge₃ precipitates or both,⁸ which is of interest for composite magnetic semiconductor applications.

At present, the exact nature of the Ge_{1-x}Mn_x nanoclusters and a microscopic explanation of the observed magnetism are unresolved issues. An atomic-scale investigation of these nanometer-sized regions embedded in a crystalline matrix by nanostructural imaging techniques such as transmission electron microscopy (TEM) is hampered by the difficulty to eliminate signals stemming from the embedding Ge matrix. Complementary information is expected from x-ray absorption (XA) spectroscopy, which is inherently element selective and influenced by the local electronic structure and the charge state of the Mn impurities in the Ge matrix. Furthermore, by utilizing circularly polarized photons we can examine the x-ray magnetic circular dichroism (XMCD) resulting from magnetically active Mn impurities.

In this letter, we compare samples with varying amounts of Ge_{1-x}Mn_x nanoclusters and Mn₅Ge₃ precipitates through

their XA and XMCD spectra at the Mn *L*-edge. We show that Ge_{1-x}Mn_x nanoclusters exhibit a reduced average magnetic response compared to Mn₅Ge₃ precipitates in epitaxial thin films with equal total Mn content. In spite of these differences, XA spectroscopy (XAS) indicates a very similar local electronic and structural environment for Mn incorporated in Ge_{1-x}Mn_x and intermetallic Mn₅Ge₃, respectively.

The thin films investigated in this work were fabricated by solid source low temperature molecular beam epitaxy on Ge(001) substrates. Details on the fabrication procedure are given in Refs. 4 and 8. All thin films were grown with a Ge flux rate of $r_{\text{Ge}}=0.08 \text{ \AA s}^{-1}$ and a Mn content of $x=2.8\%$.

Structural properties were measured in cross-sectional TEM with an FEI Titan 80-300 microscope, magnetic properties in a commercial Quantum Design MPMS-XL superconducting quantum interference device (SQUID). Mn contents were measured by secondary ion mass spectroscopy using a Mn implanted standard. XA measurements at the Mn *L*-edge were carried out at the beamline 4.0.2 (Ref. 9) of the Advanced Light Source in the bulk sensitive¹⁰ total fluorescence yield (TFY) mode. XMCD spectra were acquired in a magnetic field of 0.5 T applied collinear with the x-ray beam and at an angle of 30° to the sample surface. Prior to the measurement, the thin film surfaces were cleaned from Ge oxides by a deionized water dip.¹¹

Three thin films, fabricated at substrate temperatures of $T_s=60, 85, \text{ and } 120 \text{ }^\circ\text{C}$, are presented in this letter. The epitaxy was found to be controllable with the fabrication temperature. At $T_s=60 \text{ }^\circ\text{C}$, thin films consist solely of self-assembled Mn-rich Ge_{1-x}Mn_x nanoclusters embedded in a Ge matrix with diamond-type lattice.⁴ Increasing the fabrication temperature beyond 60 °C additionally leads to the precipitation of nanometer-sized inclusions of the intermetallic compound Mn₅Ge₃ in the Ge matrix.⁸ This is shown in Fig. 1, where a cross-sectional TEM overview image of the $T_s=85 \text{ }^\circ\text{C}$ thin film is depicted. The image shows a dense assembly of nanometer-sized, elongated regions of dark con-

^{a)}Electronic mail: bougeard@wsi.tum.de.

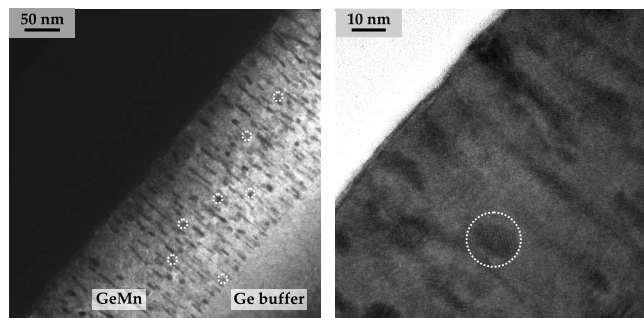


FIG. 1. Cross-sectional TEM images. (left) Overview image and (right) close-up image. White dashed circles mark regions exhibiting Moiré patterns.

trast corresponding to self-assembled $\text{Ge}_{1-x}\text{Mn}_x$ nanoclusters. In addition several approximately round regions, indicated by the white dashed circles, are visible. These regions correspond to Mn_5Ge_3 precipitates with hexagonal $D8_8$ lattice structure.⁷ In a higher magnification image these regions exhibit Moiré-patterns, which are due to a crystal structure differing from the surrounding Ge matrix with diamond-type lattice. Increasing the fabrication temperature further increases the amount of the Mn_5Ge_3 precipitates while the amount of self-assembled $\text{Ge}_{1-x}\text{Mn}_x$ nanoclusters decreases. At $T_S=120^\circ\text{C}$, only Mn_5Ge_3 precipitates are observed. In the temperature range of $60^\circ\text{C} \leq T_S \leq 120^\circ\text{C}$, the appearance of the thin films thus gradually changes from the exclusive presence of self-assembled $\text{Ge}_{1-x}\text{Mn}_x$ nanoclusters at $T_S=60^\circ\text{C}$ to a composite material containing both $\text{Ge}_{1-x}\text{Mn}_x$ nanoclusters and inclusions of intermetallic Mn_5Ge_3 at $T_S=85^\circ\text{C}$. Eventually, at $T_S=120^\circ\text{C}$, only Mn_5Ge_3 precipitates are present. Note that the total Mn content of the epitaxial film was not changed from film to film.

XAS spectra of the thin films acquired at the Mn $L_{3,2}$ edge are shown in Figs. 2(a) and 2(b). The absorption spectrum of the $T_S=60^\circ\text{C}$ $\text{Ge}_{1-x}\text{Mn}_x$ nanocluster thin film exhibits broad L_2 and L_3 peaks without a pronounced fine structure. XAS line shapes and $L_{3,2}$ absorption peak energies serve as a fingerprint for the electronic and structural configuration of the material under investigation. However, in spite of distinctively different crystal structure and chemical composition of $\text{Ge}_{1-x}\text{Mn}_x$ nanoclusters and Mn_5Ge_3 precipitates,^{4,8} the transition from solely $\text{Ge}_{1-x}\text{Mn}_x$ nanoclusters at $T_S=60^\circ\text{C}$ to solely Mn_5Ge_3 precipitates at $T_S=120^\circ\text{C}$ does not alter the XAS line shape nor results in a chemical shift in the $L_{3,2}$ energetic positions. All spectra resemble that of metallic Mn both in line shape and $L_{3,2}$ branching ratio, indicating the presence of metallic, delocalized $3d$ states of the absorbing Mn atoms in all thin films.^{12–14}

The fact that the thin films exhibit a common XAS fingerprint is further illustrated in Fig. 2(b), where the spectra of all thin films were scaled to match the L_3 peak intensity of the $T_S=120^\circ\text{C}$ thin film. Clearly, only the intensity of the spectra is decreased as the content in $\text{Ge}_{1-x}\text{Mn}_x$ nanoclusters is increased with decreasing T_S , demonstrated by the different scaling factors denoted in the figure.

The similarity in the XAS fingerprints indicates a strong similarity in the electronic configuration of the Mn atoms incorporated in $\text{Ge}_{1-x}\text{Mn}_x$ nanoclusters and Mn_5Ge_3 precipitates, respectively. In particular charge state and—as far as the resulting spectral shape is not washed out due to the delocalized $3d$ electrons—also the local coordination of the

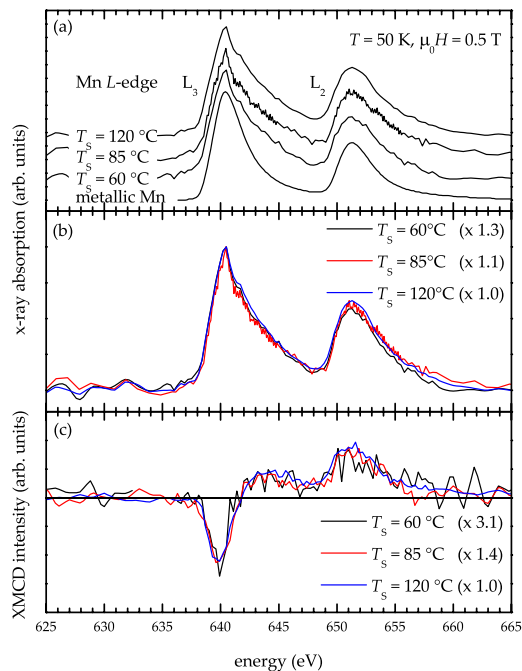


FIG. 2. (Color online) XAS [(a) and (b)] and corresponding XMCD spectra (c) of GeMn thin films measured at 50 K. The total Mn content for all films is 2.8%. For comparison, the absorption spectrum of metallic Mn is included in (a) (Ref. 15). The XAS and XMCD spectra are normalized to the L_3 peak intensity of the $T_S=120^\circ\text{C}$ thin film in [(b) and (c)], respectively. The scaling factors are given in the figures.

absorbing Mn in $\text{Ge}_{1-x}\text{Mn}_x$ nanoclusters and Mn_5Ge_3 precipitates are indistinguishable within the resolution of the measurement.

In order to investigate the magnetic activity of the incorporated Mn atoms, XMCD spectra were measured and are shown in Fig. 2(c). At $T_S=60^\circ\text{C}$, three broad peaks are observed in the XMCD spectrum. These three features are clearly distinguishable in spite of the small signal to noise ratio of the spectra. As in the case of the XAS spectra, the XMCD spectra are indicative of metallic, delocalized Mn $3d$ states. Again, the transition from $\text{Ge}_{1-x}\text{Mn}_x$ nanoclusters to Mn_5Ge_3 precipitates does not alter the line shape of the XMCD spectra. However, the intensities of all three XMCD peaks decrease with increasing amount of $\text{Ge}_{1-x}\text{Mn}_x$ nanoclusters. The XMCD spectra shown in Fig. 2(c) are scaled to match the L_3 XMCD intensity of the $T_S=120^\circ\text{C}$ thin film and superimpose within the experimental error. The scaling factors are given in the figure. It is interesting to note that, according to the relative spin and orbital moment sum rules,¹⁶ the scalability of the XMCD spectra translates into similar ratios of the spin and orbital moments of Mn incorporated in $\text{Ge}_{1-x}\text{Mn}_x$ nanoclusters and in Mn_5Ge_3 precipitates. Furthermore the scaling factors of the XAS and XMCD spectra infer a decreased average magnetic moment per Mn when $\text{Ge}_{1-x}\text{Mn}_x$ nanoclusters are introduced and their amount is increased at the expense of Mn_5Ge_3 precipitates.

This latter finding is corroborated by field dependent magnetization loops, recorded with conventional SQUID magnetometry and depicted in Fig. 3. In spite of an identical total Mn content in the three thin films, they display increasing magnetization with increasing fabrication temperature. The presence of $\text{Ge}_{1-x}\text{Mn}_x$ nanoclusters in the $T_S=60$ and 85°C thin films, thus leads to reduced magnetic response compared to the $T_S=120^\circ\text{C}$ film containing only Mn_5Ge_3

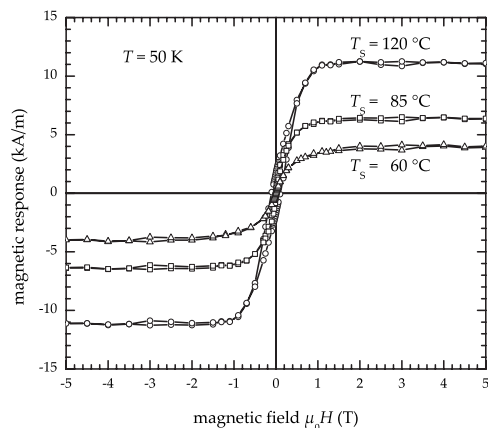


FIG. 3. SQUID magnetization loops measured at 50 K.

precipitates. Since all samples contain the same total amount of Mn atoms, SQUID measurements also infer a reduced average magnetic moment per Mn atom when the amount of $\text{Ge}_{1-x}\text{Mn}_x$ nanoclusters is increased at the expense of Mn_5Ge_3 precipitates.

In our study XAS indicates an experimentally indistinguishable charge state and local coordination of Mn in all samples. XMCD underpins this similarity through an equal ratio of orbital and spin moment. At the same time, both XMCD as well as SQUID magnetometry measurements show that when increasing the amount of $\text{Ge}_{1-x}\text{Mn}_x$ nanoclusters at the expense of Mn_5Ge_3 precipitates, the magnetic response of the thin films decreases. These apparently opposing observations of a differing Mn magnetic moment with at the same time, strong similarities in the Mn electronic environment and magnetic configuration leads to the conclusion that not every individual Mn atom contributes to the measured magnetic response. Although being element-specific, XA such as SQUID magnetometry delivers an information averaged over the total sample volume. We thus conclude that, while all Mn atoms exhibit similar atomic magnetic moments, a fraction of the atoms is magnetically inactive and therefore not contributing to the measured XMCD and SQUID magnetic response. The amount of the magnetically inactive Mn increases with the presence of nanoclusters and is highest in the absence of Mn_5Ge_3 precipitates at $T_S = 60^\circ\text{C}$, hinting toward a relationship between the presence of nanoclusters and of a fraction of Mn atoms which do not contribute to the total magnetization.

Magnetic inactivity not only in $\text{Ge}_{1-x}\text{Mn}_x$ but also in other magnetic semiconductors may have various origins. These can be antiferromagnetic interaction between Mn atoms leading to magnetic frustration¹⁷ and spin disorder.¹⁸ They can also be Mn 3d states forming a low or zero moment, metallic impurity band as it was recently found in amorphous $\text{Si}_{1-x}\text{Mn}_x$.¹⁵ The latter represents a noteworthy explanation for the magnetic inactivity observed in this work, since delocalized, metallic 3d states were indeed found in the XAS fingerprints presented in Fig. 2. Remarkably, hints for crystallographic disorder can be found in reports on epitaxially fabricated GeMn free of Mn_5Ge_3 precipitates.^{1,2,19,20} It will therefore be interesting to investigate the next-nearest neighbor coordination shells of the Mn atoms, for instance by extended XA fine structure analysis, in order to clarify the presence of such structural disorder and

to ascertain to what extent disorder leads to the observed magnetic inactivity.

In summary, the combination of XAS, electron microscopy and magnetometry reveals a strong similarity of the Mn incorporation in $\text{Ge}_{1-x}\text{Mn}_x$ nanoclusters and in Mn_5Ge_3 precipitates. This close relationship suggests similar magnetic moments of the magnetically active Mn atoms contributing to the overall magnetization. The observed reduced average magnetic response of the thin films containing $\text{Ge}_{1-x}\text{Mn}_x$ nanoclusters is expected to be due to a certain fraction of magnetically inactive Mn atoms. Structural disorder stemming from $\text{Ge}_{1-x}\text{Mn}_x$ nanoclusters is considered as a noteworthy explanation for the observed magnetic inactivity. Investigating crystallographic disorder therefore appears to be an important and instructive task for further engineering of this promising magnetic semiconductor.

This work was funded by the German Science Foundation (DFG) via Schwerpunktprogramm SPP 1285 Halbleiter Spintronik and supported by the U.S. Department of Energy under Contract No. DE-AC02-05CH11231. The authors acknowledge access to facilities of the Nanosystems Initiative Munich (NIM) and the Department of Chemistry, Technische Universität München, and support by M. Döblinger, T. F. Fässler, M. B. Boeddinghaus, R. Farshchi, and S. Tardif. P.R.S. is furthermore grateful for support from NSF and NDSEG and D.B. for support by Alexander von Humboldt-Stiftung.

¹M. Jamet, A. Barski, T. Devillers, V. Poydenot, R. Dujardin, P. Bayle-Guillemaud, J. Rothman, E. Bellet-Amalric, A. Marty, J. Cibert, R. Matana, and S. Tatarenko, *Nature Mater.* **5**, 653 (2006).

²A. P. Li, C. Zeng, K. van Benthem, M. F. Chisholm, J. Shen, S. V. S. N. Rao, S. K. Dixit, L. C. Feldman, A. G. Petukhov, M. Foygel, and H. H. Weitering, *Phys. Rev. B* **75**, 201201(R) (2007).

³C. Zeng, Z. Zhang, K. van Benthem, M. F. Chisholm, and H. H. Weitering, *Phys. Rev. Lett.* **100**, 066101 (2008).

⁴D. Bougeard, S. Ahlers, A. Trampert, N. Sircar, and G. Abstreiter, *Phys. Rev. Lett.* **97**, 237202 (2006).

⁵Y. Tawara and K. Sato, *J. Phys. Soc. Jpn.* **18**, 773 (1963).

⁶N. Yamada, *J. Phys. Soc. Jpn.* **59**, 273 (1990).

⁷J. B. Forsyth and P. J. Brown, *J. Phys.: Condens. Matter* **2**, 2713 (1990).

⁸S. Ahlers, D. Bougeard, N. Sircar, G. Abstreiter, A. Trampert, M. Opel, and R. Gross, *Phys. Rev. B* **74**, 214411 (2006).

⁹E. Arenholz and S. O. Prestemon, *Rev. Sci. Instrum.* **76**, 083908 (2005).

¹⁰Y. Idzerda, C. Chen, H.-J. Lin, G. Meigs, G. Ho, and C.-C. Kao, *Nucl. Instrum. Methods Phys. Res. A* **347**, 134 (1994).

¹¹S. Rivillon, Y. J. Chabal, F. Amy, and A. Kahn, *Appl. Phys. Lett.* **87**, 253101 (2005).

¹²P. De Padova, J. P. Ayoub, I. Berbezier, P. Perfetti, C. Quaresima, A. M. Testa, D. Fiorani, B. Olivieri, J. M. Mariot, A. Taleb-Ibrahimi, M. C. Richter, O. Heckmann, and K. Hricovini, *Phys. Rev. B* **77**, 045203 (2008).

¹³P. Gambardella, L. Claude, S. Rusponi, K. J. Franke, H. Brune, J. Raabe, F. Nolting, P. Bencok, A. T. Hanbicki, B. T. Jonker, C. Grazioli, M. Veronese, and C. Carbone, *Phys. Rev. B* **75**, 125211 (2007).

¹⁴L. Sangaletti, D. Ghidoni, S. Pagliara, A. Goldoni, A. Morgante, L. Floreano, A. Cossaro, M. C. Mozzati, and C. B. Azzoni, *Phys. Rev. B* **72**, 035434 (2005).

¹⁵L. Zeng, A. Huegel, E. Helgren, F. Hellman, C. Piamonteze, and E. Arenholz, *Appl. Phys. Lett.* **92**, 142503 (2008).

¹⁶C. T. Chen, Y. U. Idzerda, H.-J. Lin, N. V. Smith, G. Meigs, E. Chaban, G. H. Ho, E. Pellegrin, and F. Sette, *Phys. Rev. Lett.* **75**, 152 (1995).

¹⁷K. W. Edmonds, N. R. S. Farley, T. K. Johal, G. van der Laan, R. P. Campion, B. L. Gallagher, and C. T. Foxon, *Phys. Rev. B* **71**, 064418 (2005).

¹⁸G. Zaránd and B. Jankó, *Phys. Rev. Lett.* **89**, 047201 (2002).

¹⁹M. Rovezzi, T. Devillers, E. Arras, F. d'Acapito, A. Barski, M. Jamet, and P. Pochet, *Appl. Phys. Lett.* **92**, 242510 (2008).

²⁰S. Sugahara, K. Lee, S. Yada, and M. Tanaka, *Jpn. J. Appl. Phys., Part 2* **44**, L1426 (2005).